

# High Gamma-Aminobutyric Acid (GABA) Oolong Tea Alleviates High-Fat Diet-Induced Metabolic Disorders in Mice

Published as part of the ACS Omega virtual special issue "Phytochemistry".

Monthana Weerawatanakorn, Sang He, Chun-Han Chang, Yen-Chun Koh, Meei-Ju Yang, and Min-Hsiung Pan\*

Cite This: *ACS Omega* 2023, 8, 33997–34007

Read Online

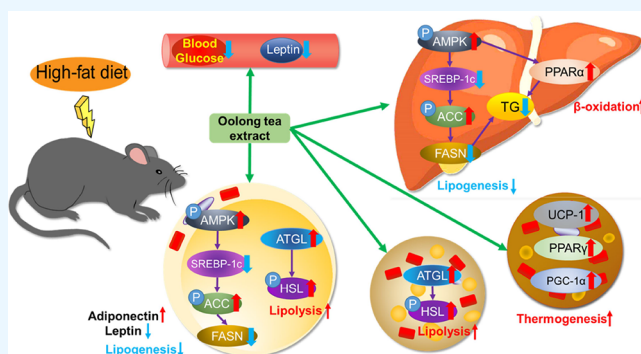
ACCESS |

Metrics & More

Article Recommendations

Supporting Information

**ABSTRACT:** Obesity and overweight are associated with an increasing risk of developing health conditions and chronic non-communicable diseases, including cardiovascular diseases, cancer, musculoskeletal problems, respiratory problems, and mental health, and its prevalence is rising. Diet is one of three primary lifestyle interventions. Many bioactive components in tea especially oolong tea, including flavonoids, gamma-aminobutyric acid (GABA), and caffeine were reported to show related effects in reducing the risk of obesity. However, the effects of GABA oolong tea extracts (OTEs) on high-fat diet (HFD)-induced obesity are still unclear. Therefore, this study aims to explore whether the intervention of GABA OTEs can prevent HFD-induced obesity and decipher its underlying mechanisms using male C57BL/6 J mice. The result indicated that GABA OTEs reduced leptin expression in epididymal adipose tissue and showed a protective effect on nonalcoholic fatty liver disease. It promoted thermogenesis-related protein of uncoupling protein-1 and peroxisome proliferator-activated receptor-gamma coactivator (PGC-1 $\alpha$ ), boosted lipid metabolism, and promoted fatty acid oxidation. It also reduced lipogenesis-related protein levels of sterol regulatory element binding protein, acetyl-CoA carboxylase, and fatty acid synthase and inhibited hepatic triglyceride (TG) levels. These data suggest that regular drinking of GABA oolong tea has the potential to reduce the risk of being overweight, preventing obesity development through thermogenesis, lipogenesis, and lipolysis.



## 1. INTRODUCTION

The prevalence of obesity has tripled over the last 40 years from 1976 to 2016.<sup>1</sup> More than 1 billion people worldwide are obese with 650 million adults, 340 million adolescents, and 39 million children (WHO 2022). The causes of obesity are very complex, including genetic, physiological, environmental, behavioral, psychological, and even political factors.<sup>2</sup> The worldwide epidemic of obesity by WHO is an abnormal or excessive fat accumulation that damages our health, and it is the major risk factor for the development of many chronic non-communicable diseases, such as diabetes, hypertension, stroke, cardiovascular disease, and cancer.<sup>3</sup>

White adipocyte expansion leads to obesity, however, it can transdifferentiate into beige and brown adipocytes. Brown adipocytes reside in specific depots called brown adipose tissues (BATs) containing numerous smaller lipid droplets and more mitochondria, and it produces heat by non-shivering thermogenesis.<sup>4</sup> Therefore, it is believed that white adipose tissue (WAT) browning is one key to treating obesity and its associated metabolic diseases. Obesity is also associated with alterations in the hormone levels, such as adiponectin and

leptin, while the leptin/adiponectin ratio is considered a more accurate predictor of obesity.<sup>5</sup> Adiponectin plays an important role in type 2 diabetes and obesity,<sup>6</sup> and leptin is also related to inflammation and metabolic diseases,<sup>7</sup> such as adipose tissue expansion and liver steatosis.<sup>8</sup> Obese patients usually have lower adiponectin levels and higher leptin levels in both adipose tissue and serum.<sup>9</sup> Besides, adipose tissue inflammation can also cause the development of nonalcoholic fatty liver disease (NAFLD).<sup>10</sup> Excessive accumulation and less excretion of triglycerides (TGs) are the causes of NAFLD, and some proteins, such as sterol regulatory element binding protein (SREBP-1c), acetyl-CoA carboxylase (ACC1), fatty acid synthase (FASN), and peroxisome proliferator-activated receptor alpha (PPAR $\alpha$ ), are closely related to NAFLD.<sup>11</sup>

Received: July 7, 2023

Accepted: August 16, 2023

Published: September 5, 2023



There is an increase in oolong tea consumption for health promotion. Oolong tea possesses many pharmacological activities, such as antioxidant activity, anti-cancer, anti-obesity, anti-diabetes, anti-allergy, and anti-septic, and preventive effects of atherosclerosis and hypertension.<sup>12</sup> It was reported on slowing body weight gain compared to green tea, black tea, and white tea.<sup>13</sup> Oolong tea extracts (OTEs) regulate lipid metabolism and modulate gut microbiota through high levels of flavonoids. Tea flavonoids decrease lipogenesis-related protein SREBP-1 and FASN expression and promote thermogenesis-related protein expression in epididymal adipose tissue.<sup>14</sup>

Besides flavonoid, all types of teas contain modest amounts of  $\gamma$ -aminobutyric acid (GABA), a neurotransmitter lead to induce relaxation and diminish anxiety,<sup>15</sup> but few pieces of literature studies have explored its effect on obesity. There is an anaerobic process that increases GABA in tea by 10–20 times.<sup>15</sup> A cup of GABA-fortified oolong tea containing 1.05 mg/100 mL significantly reduced autonomic imbalance and heart rate variability with acute stress.<sup>16</sup> In addition, caffeine in tea promotes fat loss through the activation of adenosine 5'-monophosphate (AMP)-activated protein kinase (AMPK), inhibits lipogenesis protein expression of SREBP-1c and FASN protein expressions leading to inhibit lipogenesis,<sup>17,18</sup> stimulates thermogenesis in BAT,<sup>19</sup> and increases fat oxidation.<sup>20</sup> Therefore, we investigate the effects of GABA OTEs on the anti-obesity using a high-fat diet (HFD) C57BL/6 J mice model. Many proteins and genes related to signaling pathways in adipose tissue were studied to explore the obesity protective mechanism of GABA OTEs.

## 2. MATERIALS AND METHODS

**2.1. Chemicals and Drugs.** The ACC, AMPK $\alpha$ , p-AMPK $\alpha$ ,  $\alpha/\beta$ -tubulin, hormone-sensitive lipase (HSL), p-HSL, and uncoupling protein-1 (UCP-1) primary antibodies were purchased from Cell Signaling Technology (Beverly, MA, US). The peroxisome proliferator-activated receptor gamma (PPAR $\gamma$ ), PPAR $\alpha$ , glyceraldehyde-3-phosphate dehydrogenase (GAPDH), leptin, adiponectin, and proliferator-activated receptor-gamma coactivator (PGC-1 $\alpha$ ) primary antibodies were purchased from Abcam (Cambridge, UK). The Vinculin antibody was purchased from Proteintech (IL, US). The  $\beta$ -actin antibody was purchased from Sigma Chemical Co (MA, US). The p-ACC, SREBP-1, and adipose triglyceride lipase (ATGL) antibodies were purchased from Santa Cruz (Texas, US). The nutraceuticals component of GABA oolong tea was determined, and the result is presented in Table 1

**2.2. High-GABA OTE Preparation.** OTEs were provided by the Taiwan Tea Research and Extension Station (Taoyuan, Taiwan). The tea tree variety used for the oolong tea is TTES No.17 bred by Taiwan Tea Research and Extension Station since 1983. The prepared oolong tea leaves were water extracted according to the procedures of making tea. The tea was freeze-dried into OTE and stored at  $-20\text{ }^{\circ}\text{C}$  before further analysis.

**2.3. Animals and Experimental Design.** Four-week-old male C57BL/6 J mice were purchased from the National Laboratory Animal Center. The mice were housed in a room at  $23 \pm 3\text{ }^{\circ}\text{C}$  with  $50 \pm 10\%$  relative humidity and 12 h of light/dark cycle. Four mice were housed in a cage with free access to Laboratory Rodent Diet 5001 and water for 1 week. All experimental protocols used in this study were approved by the Institutional Animal Care and Use Committee of the National

**Table 1. Oolong Nutraceuticals Components<sup>a</sup>**

nutraceuticals (0.2 g of GABA tea in 100 mL of water)	nutraceutical contents ( $\mu\text{g}/\text{mL}$ )
GABA	14.27
L-theanine	15.57
caffeine	180.29
C	2.06
CG	1.21
GC	4.62
EGC	27.90
EC	4.97
ECG	3.15
EGCG	12.37

<sup>a</sup>C, catechin; CG, catechin gallate; GC, gallic catechin; EGC, epigallocatechin; EC, epicatechin; ECG, epicatechin gallate; EGCG, epigallocatechin gallate.

Taiwan University (NTU-109-EL-00147, IACUC, NTU). After 1 week of adaptation, the mice were divided into three groups ( $n = 8$  per group) fed with a chow diet (ND, 13.5% calories as fat), HFD (50% calories as fat), and HFD supplemented with 1% OTE (HFD + OTE, 50% calories as fat), respectively. Food consumption, water intake, and body weight were recorded weekly. After continuing to feed for another 14 weeks, all animals were sacrificed by  $\text{CO}_2$  asphyxiation. The physical appearances of mice were immediately photographed after being sacrificed, and the blood, epididymal fat, inguinal fat, scapular brown fat, liver, spleen, and kidney were immediately collected, weighed, and photographed.

**2.4. Dosage Selection and Conversion for Human Intake.** For the dosage selection, 1% OTE was chosen as the treatment dose based on two criteria. It was previously reported that 0.5–2% of the tea extracts were commonly used as the treatment dosages [1; 2; 3]. The second criterion was to maximize the amount of GABA intake but do not exceed the maximum suggestion for caffeine, 1% was the most suitable supplementation percentage. Around 0.18 mg GABA was received by each mouse (30 g in body weight) for each day at this dosage.

In this experiment, each mouse consumed around 2–3 grams of feeding per day. In other words, around 25 mg of the sample was taken by each mouse (around 30 grams of body weight). After conversion, the dosage of the supplements given to an adult will be 4 g/60 kg body weight/day. The gross weight of vitamin supplementation tablets could reach 1 g per tablet. Therefore, it is needed to consume four tablets of our extract per day, and it is achievable in humans. In addition, our high-GABA OTE is expected to be developed into an instant tea drink. Besides, the caffeine amount in 4 g of our extract is around 360 mg, and it is generally agreed that 300–400 mg of caffeine can be consumed daily without any adverse effects. GABA (28mg) will be consumed from 4 g of the extract.

**2.5. Histological Analysis.** To make paraffin sections, the epididymal fat, inguinal fat, and liver tissue were fixed in 10% buffered formalin and dehydrated. Fixed tissues were embedded in paraffin subsequently. The liver was sliced at a thickness of 5  $\mu\text{m}$ , and the epididymal fat and inguinal fat were sliced at a thickness of 3  $\mu\text{m}$ . All the slices should be placed in 45  $^{\circ}\text{C}$  water to remove the wax, then placed in a 56  $^{\circ}\text{C}$  incubator to dry overnight to melt the residual wax. After that, stained the tissues with hematoxylin and eosin (H&E), then observation

Table 2. Primer Sequences Used for Real-Time Quantitative Reaction

primer	sequence (5'–3')	annealing temperature (°C)	ref
GAPDH F	TGGTGAAGGTCGGTGTGAAC	53.8	DOI: 10.3389/fchar.2018.00183
GAPDH R	AATGAAGGGGTCGTTGATGG	51.8	DOI: 10.3389/fphar.2018.00183
SREBP-1c F	GGCTATCCGTGAACATCTCCTA	55.3	DOI: 10.1371/journal.pone.0051007
SREBP-1c R	ATCCAAGGCATCTGAGAACTC	54.8	DOI: 10.1371/journal.pone.0051007
ACC1 F	GCTATGGAAGTCGGCTATGAAATTG	58	DOI: 10.1177/0748730405275952
ACC1 R	TCAGGAAGAGGCOGATGGGAATTG	59.1	DOI: 10.1177/0748730405275952
FASN F	GCAGCTGTTGGTTTGTCTCTG	53.8	self design
FASN R	ATTCAGTGCAGCCTGAGGTC	53.8	self design
PPAR $\alpha$ F	ACAAGCCCTCAGGGTACCA	53.2	DOI: 10.1074/jbe.M113.526.343
PPAR $\alpha$ R	GCCGAAAGAAGCCCTTACAG	53.8	DOI: 10.1074/jbe.M113.526.343

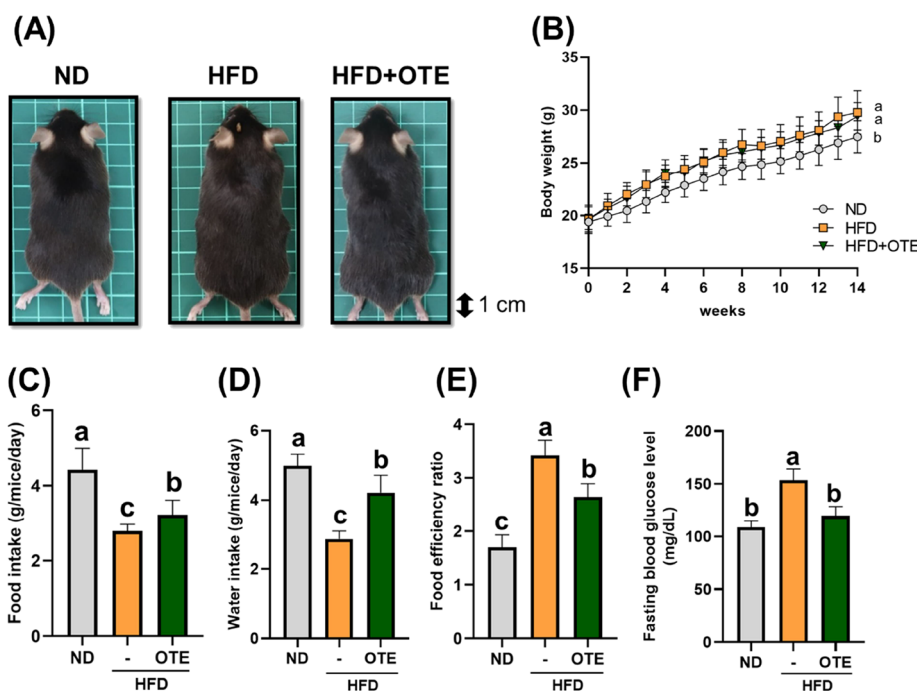


**Figure 1.** Effects of OTE supplementation on HFD-fed C57BL/6 mice. (A) Photographs of representative mice from each group at the end of treatment, (B) growth curve of mice aged 5 weeks at start, (C) food intake, (D) water intake, (E) food efficiency ratio, and (F) fasting blood glucose level measured by a glucose meter. Data are expressed as the means  $\pm$  SD ( $N = 8$ ). Differences were analyzed by one-way ANOVA and Duncan's multiple-range tests. The values with different letters (a–c) are significantly different ( $p < 0.05$ ) between each group.

and shooting in photomicroscopic. Liver and epididymal fat were measured at 200 $\times$  magnification, and inguinal fat was measured at 400 $\times$  magnification.

**2.6. Biochemical Analysis and the Fasting Glucose Test.** In this study, Elisa kits were used to evaluate adiponectin (Item No. 108785, Abcam, Cambridge, UK) and leptin (Cat. # EZML-82K, EMD Millipore Corporation, MS, US) in serum collected via cardiac puncture after sacrificing. TG in the liver was measured using a TG colorimetric assay kit (Item No. 10010303, Cayman Chemical, MI, US). Blood samples were harvested from the tail vein at 12 weeks, and the blood glucose was measured using a glucometer (Aurum Biomedical Technology, Taiwan).

**2.7. Western Blot Analysis.** Total epididymal adipose, inguinal adipose, scapular brown adipose, and liver samples were obtained for western blot analysis. Frozen tissue was homogenized for 30 s in lysis buffer supplemented with a protease inhibitor cocktail. Samples were lysed for 1 h on ice with periodic mixing and centrifuged at 10,000  $\times$  g for 30 min at 4  $^{\circ}$ C, and the supernatant was collected. The whole sample

should be routinely centrifuged and collected twice for this assay. Protein concentration was determined by the Bradford method using Protein Assay Dye (Bio-Rad). Each sample was mixed with protein–dye and boiled at 100  $^{\circ}$ C for 10 min, then separated on 8–15% gels by sodium dodecyl sulfate–polyacrylamide gel electrophoresis. After electrophoresis, proteins were transferred to an immobile membrane (poly(vinylidene difluoride)) with transfer buffer for 5 h at 4  $^{\circ}$ C and blocked with a blocking solution containing 20 mM HCl for 1 h at room temperature. Antibodies were diluted in a blocking solution and incubated with membranes overnight at 4  $^{\circ}$ C. After that, each membrane was rinsed for 10 min with TPBS (0.2% Tween 20 in 1X PBS buffer) three times. Following horseradish peroxidase-conjugated secondary antibody incubation for 1 h at room temperature, blots were visualized with an enhanced chemiluminescence detection kit.

**2.8. RNA Extraction.** Total RNA was extracted from liver tissue by homogenization in TRIzol reagent (Ambion). Following RNA, DNA, and protein layer separation with chloroform, RNA was precipitated with isopropanol and

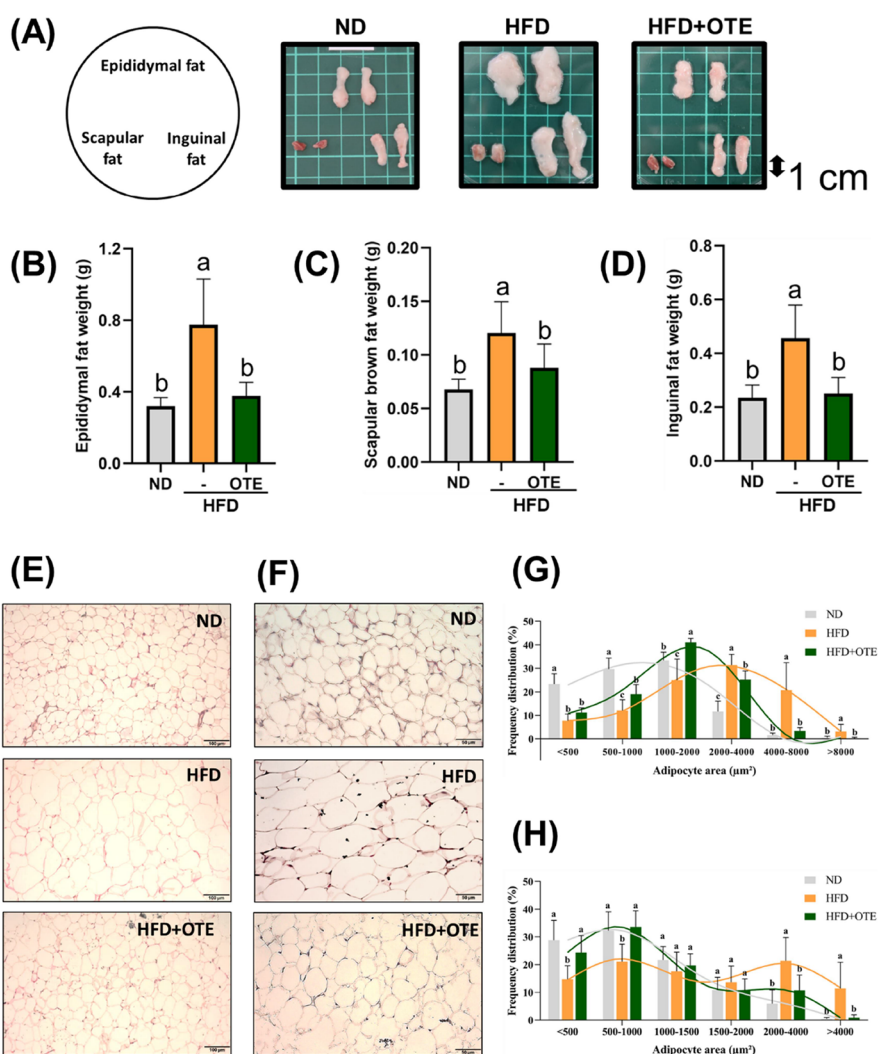


**Figure 2.** Effects of OTE supplementation on fat weight, size distribution, and histology of epididymal and inguinal adipocyte in HFD-fed C57BL/6 mice. Adipose tissues were removed and weighed immediately after being sacrificed. Epididymal and inguinal adipocyte was fixed, dehydrated, and embedded, and 3  $\mu\text{m}$  fat sections were stained with H&E stain. (A) Representative photographs of each group, (B) epididymal fat weight, (C) scapular brown fat weight, (D) inguinal adipose tissue, (E) representative images of H&E staining of paraffin sections of epididymal adipocyte (magnification: 200 $\times$ ), (F) representative images of H&E staining of paraffin sections of inguinal adipocyte (magnification: 400 $\times$ ), (G) frequency of adipocyte sizes in epididymal adipocyte, and (H) frequency of adipocyte sizes in inguinal adipocyte. Data are expressed as the means  $\pm$  SD ( $N = 8$ ). Differences were analyzed by one-way ANOVA and Duncan's multiple-range tests. The values with different letters (a–c) are significantly different ( $p < 0.05$ ) between each group.

washed with 75% EtOH. The final RNA was resuspended in diethyl pyrocarbonate water and quantified using the NanoDrop to detect its OD 260/280, OD 260/230, and RNA concentration.

The TURBO DNA-free Kit was used to digest for RNA purification before reverse transcription polymerase chain reaction. First, the RNA sample was diluted to  $<200 \text{ ng}/\mu\text{L}$ , 17  $\mu\text{L}$  of RNA sample was taken, and 2  $\mu\text{L}$  of 10X buffer and 1  $\mu\text{L}$  TURBO DNase were added. Then, the mixtures were vortexed and heated at 37  $^{\circ}\text{C}$  for 30 min. DNase inactivation reagent (2  $\mu\text{L}$ ) was added to the mixture, pipetted, and incubated at 22  $^{\circ}\text{C}$  for 5 min. The mixture was centrifuged at 10,000g for 3 min at 4  $^{\circ}\text{C}$ , and the supernatant was collected. Again, the NanoDrop was used to detect its OD 260/280, OD 260/230, and RNA concentration. OD 260/280  $> 1.6$  and OD 260/230  $> 1.6$  were accepted in this experiment.

**2.9. Real-Time Quantitative PCR.** Real-time quantitative PCR was carried out with SensiFAST SYBR No-ROX Mix kit

(Meridian Bioscience Inc) on an Applied Biosystems StepOnePlus (Thermo Fisher). Delta CT (cycle threshold)s were calculated and normalized to internal control for each sample. Primer sequences are listed in Table 2. Complimentary DNA (cDNA) was synthesized from 1  $\mu\text{L}$  of RNA by reverse transcription with SensiFast cDNA Synthesis Kit (Meridian Bioscience Inc).

**2.10. Statistical Analysis.** The results are presented as mean  $\pm$  SD. The statistical analysis was performed using SPSS, version 24 (IBM, Armonk, NY, USA). Differences between groups were statistically analyzed using one-way ANOVA and Duncan's multiple range tests and were considered statistically significant with a level of  $p$ -value  $< 0.05$ .

### 3. RESULTS

**3.1. Effect of OTE Treatment on Body Weight, Food Intake, and Water Intake in HFD-Fed C57BL/6 Mice.** A mouse model of HFD-induced obesity and hyperlipidemia was

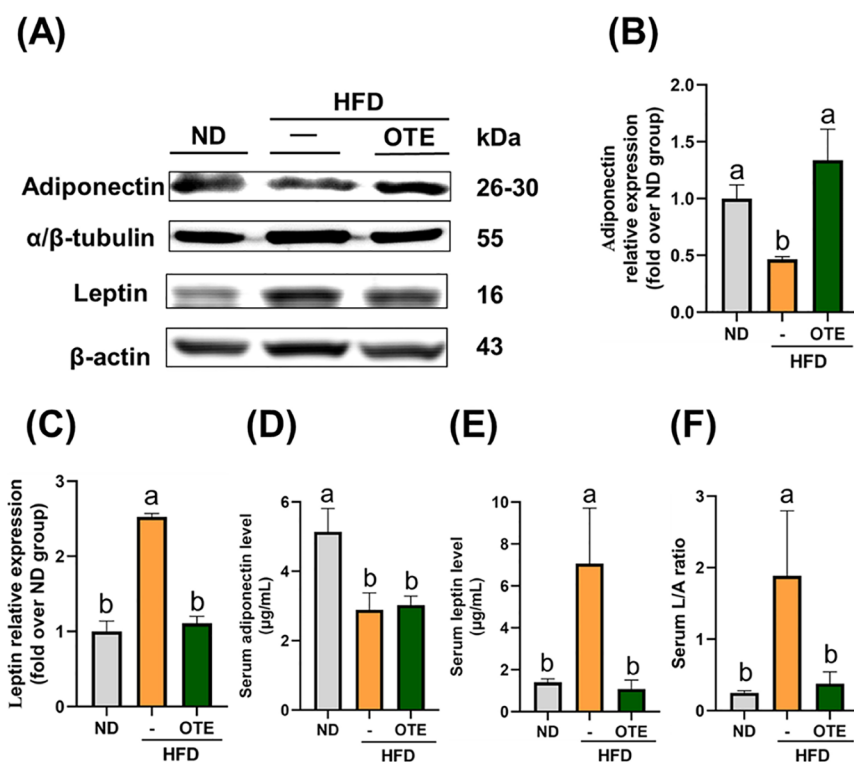


**Figure 3.** Effects of OTE supplementation on adiponectin and leptin level of epididymal adipose tissue and serum adiponectin, leptin, and serum L/A ratio in HFD-fed C57BL/6 mice. The serum was measured using a commercial kit. (A) Western blotting analysis of hormones, (B) adiponectin, (C) leptin, (D) serum adiponectin, (E) serum leptin, and (F) serum L/A ratio. Data are expressed as the means  $\pm$  SD ( $N = 4-5$  for western blot, and  $N = 8$  for serum analysis). Differences were analyzed by one-way ANOVA and Duncan's multiple-range tests. The values with different letters (a–b) are significantly different ( $p < 0.05$ ) between each group.

used. The 4-week-old C57BL/6 J mice were housed with a 12 h light–dark cycle and divided into three groups fed with ND, HFD, and HFD supplemented with 1% GABA OTEs for 14 weeks to identify the anti-obesity effect of OTE. The result shows that the HFD group was fatter in appearance and significantly heavier than the ND group, while the HFD with OTE mice were thinner than the HFD group, showing a downward trend in body weight but no significance at this time point (Figure 1A,B and Table S1). In addition, food and water consumption in HFD with OTE mice significantly increased, and the food efficiency ratio was decreased compared with the HFD group (Figure 1C–E). Moreover, we found that mice fed an HFD may develop hyperglycemia due to the high fasting blood glucose levels, while fasting blood glucose levels were ameliorated in the HFD with OTE group compared with the HFD group (Figure 1F).

**3.2. OTE Treatment Decreases the Lipid Content in Adipose Tissue in HFD-Fed C57BL/6 Mice.** We then isolated epididymal adipose tissue, inguinal adipose tissue, and scapular BAT from the mice after being sacrificed. The result showed that all three types of adipose tissue weight and size were significantly increased in the HFD group and decreased in HFD with the OTE group (Figure 2A–D). To examine whether a decrease in body fat weight changes fat cell size, an H&E staining process was needed in this experiment. The result indicated that OTE treatment dramatically reduced adipocyte size in both epididymal adipose and inguinal adipose (Figure 2E–H).

**3.3. OTE Treatment Regulates Hormone Levels in HFD-Fed C57BL/6 Mice.** Adiponectin and leptin levels are crucial for adipose tissue expansion.<sup>9</sup> Both of them secrete

from adipose tissue and then flow into the liver, inhibiting hepatic de novo lipogenesis and promoting  $\beta$ -oxidation by increasing the phosphorylation of AMPK to decrease the protein expressions of SREBP-1c and FASN.<sup>21</sup> Compared with the HFD group, HFD with the OTE group significantly improved protein expression of adiponectin and reduced leptin expression in epididymal adipose tissue (Figure 3A–C). We further measured the adiponectin and leptin levels in serum. The data revealed that HFD with OTE mice displayed a reduction of circulating leptin levels and constant adiponectin levels compared with the HFD group (Figure 3D–F).

**3.4. OTE Treatment Decreases Liver Weight and Hepatic Triglycerides Level in HFD-Fed C57BL/6 Mice.** Diet-induced obesity is usually related to NAFLD.<sup>22</sup> Mice were sacrificed after 14 weeks and the liver, kidneys, and spleens were removed for further observation. Our result showed that the appearance of the liver was markedly yellowish and was heavier in the HFD group compared with the ND group, while the dark-red color was recovered in mice with OTE treatment (Figure 4A). The weight of the kidney and spleen of the HFD group was not significantly different from other groups, but the liver weight of the HFD group was higher than others (Figure 4B–D). We further stained representative liver with H&E, and the result indicated that OTE treatment effectively inhibited hepatocellular ballooning and micro-vesicular accumulations compared with the HFD group (Figure 4F). Previous studies showed that intrahepatic TG accumulation contributed to fatty liver and even NAFLD.<sup>23</sup> As expected, the hepatic TG content in the HFD group was much higher than the ND group, and the one in the HFD with the OTE group showed a statistically significant decline (Figure 4E).

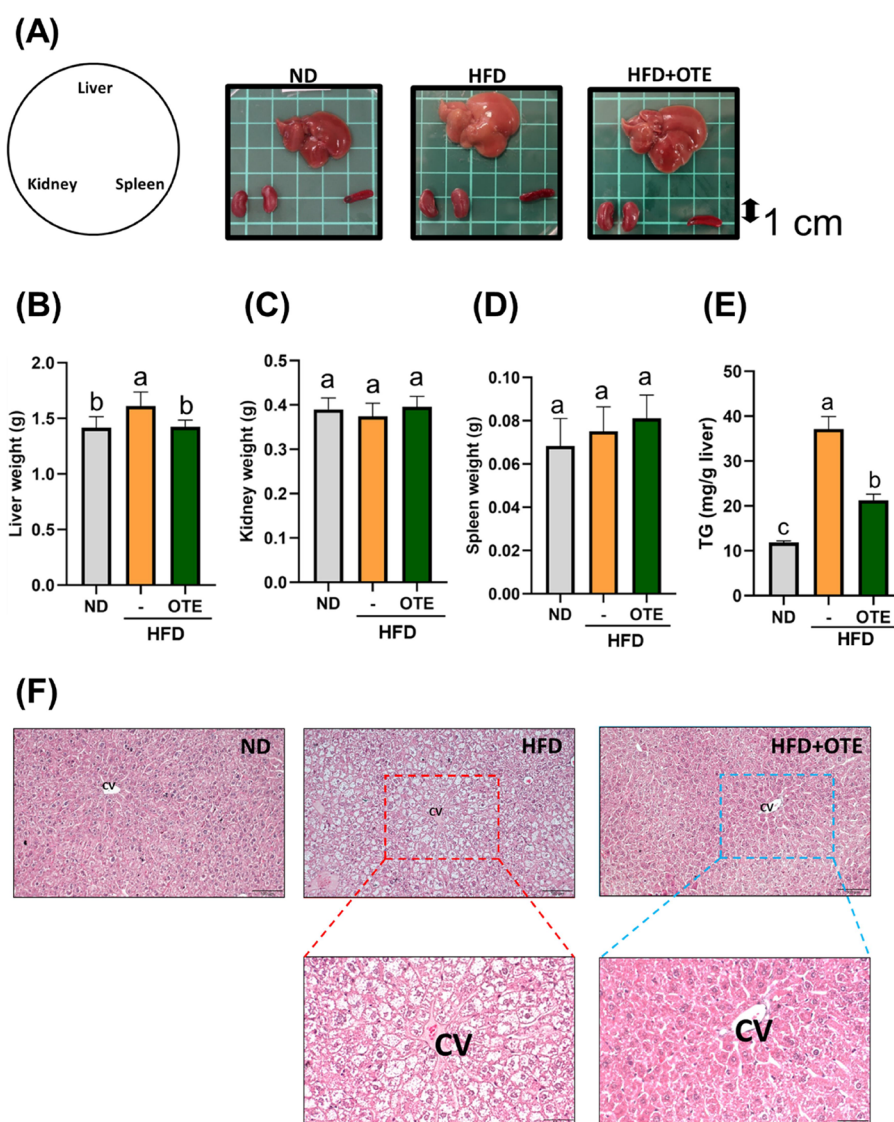


**Figure 4.** Effects of OTE supplementation on the appearance of organ, weight, liver histology, and hepatic triglycerides level in HFD-fed C57BL/6 mice. The liver, kidney, and spleen were removed and weighed immediately after sacrificed and were fixed, dehydrated, and embedded, 5  $\mu$ m liver sections were stained with H&E stain. (A) Representative photographs of each group, (B) weight of liver, (C) weight of kidney, (D) weight of spleen, (E) hepatic triglycerides level, and (F) representative images of H&E staining of paraffin sections of the liver (magnification: 200 $\times$ ). The central vein is abbreviated to CV. Data are expressed as the means  $\pm$  SD ( $N = 8$ ). Differences were analyzed by one-way ANOVA and Duncan's multiple-range tests. The values with different letters (a–c) are significantly different ( $p < 0.05$ ) between each group.

**3.5. OTE Treatment Stimulates Lipolysis of both Epididymal and Inguinal Adipose Tissue in HFD-Fed C57BL/6 Mice.** Lipolysis is a well-known metabolic pathway in which TG is hydrolyzed into glycerol and free fatty acids by the enzymes HSL and ATGL.<sup>24</sup> Our western blot analysis indicated that the protein expression of ATGL and phosphorylation of HSL showed a dramatic decline in both epididymal (Figure 5A–C) and inguinal adipose tissue (Figure 6A–C) after feeding with HFD, indicating that the mechanism of adipose tissue lipolysis may impair. In contrast, OTE treatment significantly increased the expression of ATGL and stimulate the phosphorylation of HSL in both epididymal and inguinal adipose tissue (Figures 5A–C and 6A–C). These data suggested that OTE treatment had epididymal and inguinal adipose-specific effects in boosting lipid metabolism.

**3.6. OTE Treatment Promotes Thermogenesis of Scapular Brown Adipose Tissue in HFD-Fed C57BL/6 Mice.** Thermogenesis is a unique mechanism that can produce

heat in all warm-blooded animals,<sup>25</sup> and BAT is the main site of thermogenesis to regulate our body metabolism through activating thermogenesis-related proteins, such as UCP-1 and PGC-1 $\alpha$ .<sup>26</sup> Our result showed that the thermogenesis-related proteins UCP-1 and PGC-1 $\alpha$  remained constant in the HFD group compared with the ND group but were greatly enhanced by OTE treatment (Figure 6D–F). In addition, the proliferation-related protein PPAR $\gamma$  was also increased by OTE treatment (Figure 6D,G), indicating that OTE has the potential effect to promote thermogenesis by increasing brown adipocyte number.

**3.7. OTE Treatment Inhibits Lipogenesis of Epididymal Adipose Tissue in HFD-Fed C57BL/6 Mice.** Lipogenesis is a series of reactions in which carbohydrates are converted into fatty acids, then dehydrated and condensed with glycerol to form TGs.<sup>27</sup> We found that OTE treatment significantly increased the phosphorylation of AMPK compared with the HFD group, and the elevated level of SREBP-

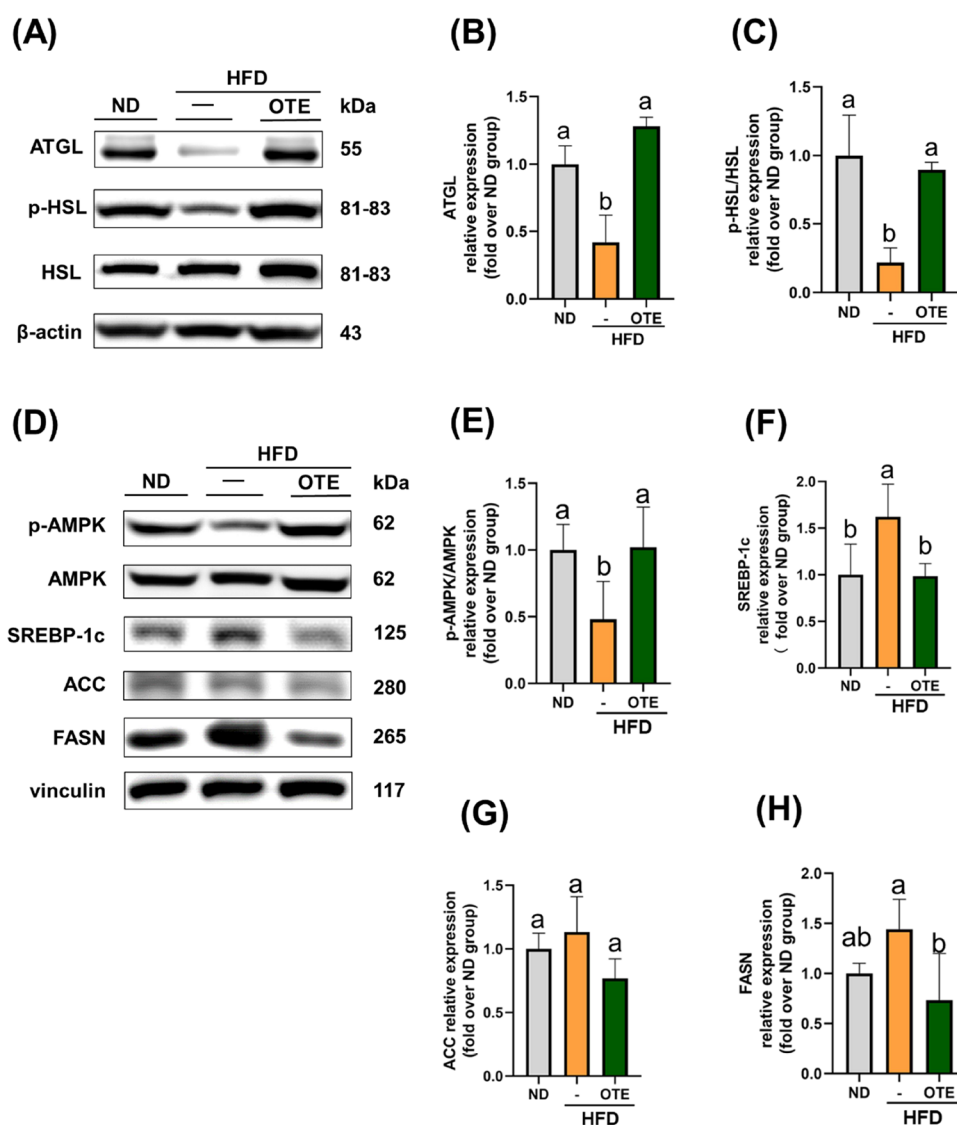


**Figure 5.** Effects of OTE supplementation on lipolysis-related proteins and lipogenesis-related proteins of epididymal adipose tissue in HFD-fed C57BL/6 mice. (A) Protein levels of epididymal adipose tissue on lipolysis-related pathways were analyzed by western blot. (B) ATGL and (C) p-HSL/HSL protein bands were quantified by Image J. (D) Protein levels of epididymal adipose tissue on lipogenesis-related pathways were analyzed by western blot. (E) p-AMPK/AMPK, (F) SREBP-1c, (G) ACC, and (H) FASN protein bands were quantified by Image J. Data are expressed as the means  $\pm$  SD ( $N = 4-5$ ). Differences were analyzed by one-way ANOVA and Duncan's multiple-range tests. The values with different letters (a–b) are significantly different ( $p < 0.05$ ) between each group.

1c, ACC, and FASN in adipocytes declined in mice with OTE treatment (Figure 5D–H). Interestingly, no bands are visible on the p-ACC blotting membranes, so we use ACC relative expression to replace p-ACC/ACC. There was no significant difference in the expression levels of ACC among the three groups, but still showed a downward trend (Figure 5G). This result suggested that ACC may hardly be phosphorylated in adipose tissue, but further investigation into p-ACC protein expression is necessary.

**3.8. OTE Treatment Inhibits Lipogenesis of the Liver in HFD-Fed C57BL/6 Mice.** Hepatic de novo lipogenesis is a crucial factor in the measurement of obesity, and the accumulation of fat in the liver may contribute to NAFLD.<sup>28</sup> We further determined the relationships between OTE and the liver to clarify the underlying mechanism. The RT-qPCR assay demonstrated that the lipogenesis-related mRNA levels of SREBP-1, ACC1, and FASN significantly declined in HFD with the OTE group compared with the HFD group (Figure

7G). Moreover, the mRNA level of PPAR $\alpha$  significantly increased in HFD with the OTE group, indicating that fatty acid oxidation may also be promoted by OTE treatment.

Consistently, the western blotting assay indicated that the protein expression levels of p-AMPK/AMPK increased in HFD with the OTE group compared with the HFD group. In the downstream protein expression of AMPK, the protein expression of SREBP-1c and FASN was inhibited in HFD with the OTE group compared with the HFD group (Figure 7A). Interestingly, the phosphorylation of ACC was increased in the HFD group compared with the ND group, and this trend continues to rise by about 10% in HFD with the OTE group (Figure 7A,D). Consistent with the trend of mRNA, OTE treatment significantly increased the protein expression of PPAR $\alpha$  compared with the HFD group, suggesting that OTE promotes fatty acid oxidation. These data illustrated that OTE can inhibit hepatic TG levels via suppressed lipogenesis and promote fatty acid oxidation.

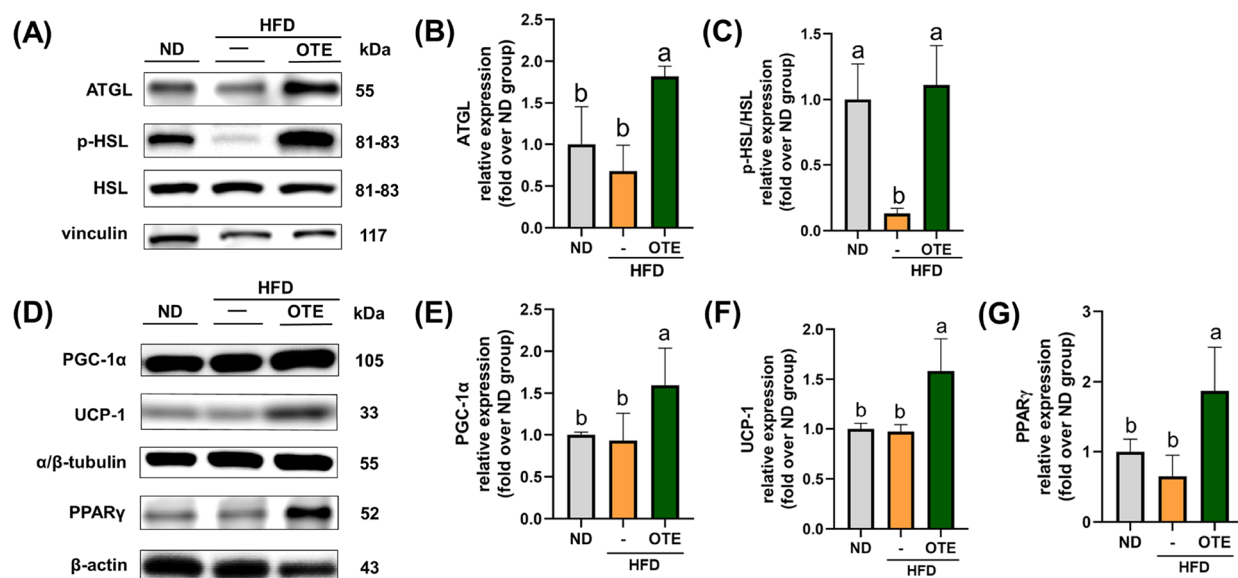


**Figure 6.** Effect of OTE supplementation on lipolysis-related proteins of inguinal adipose tissue and thermogenesis-related proteins of scapular brown adipose tissue in HFD-fed C57BL/6 mice. Protein levels were analyzed by western blot protein bands and were quantified by Image J. (A) Protein levels of inguinal adipose tissue on the lipolysis-related pathway, (B) ATGL protein band, (C) p-HSL/HSL protein bands, (D) protein levels of scapular brown adipose tissue on thermogenesis-related pathway, (E) PGC-1 $\alpha$  protein band, (F) PPAR $\gamma$  protein band, and (G) UCP-1 protein bands. Data are expressed as the means  $\pm$  SD ( $N = 4-5$  for western blot). Differences were analyzed by one-way ANOVA and Duncan's multiple-range tests. The values with different letters (a–b) are significantly different ( $p < 0.05$ ) between each group.

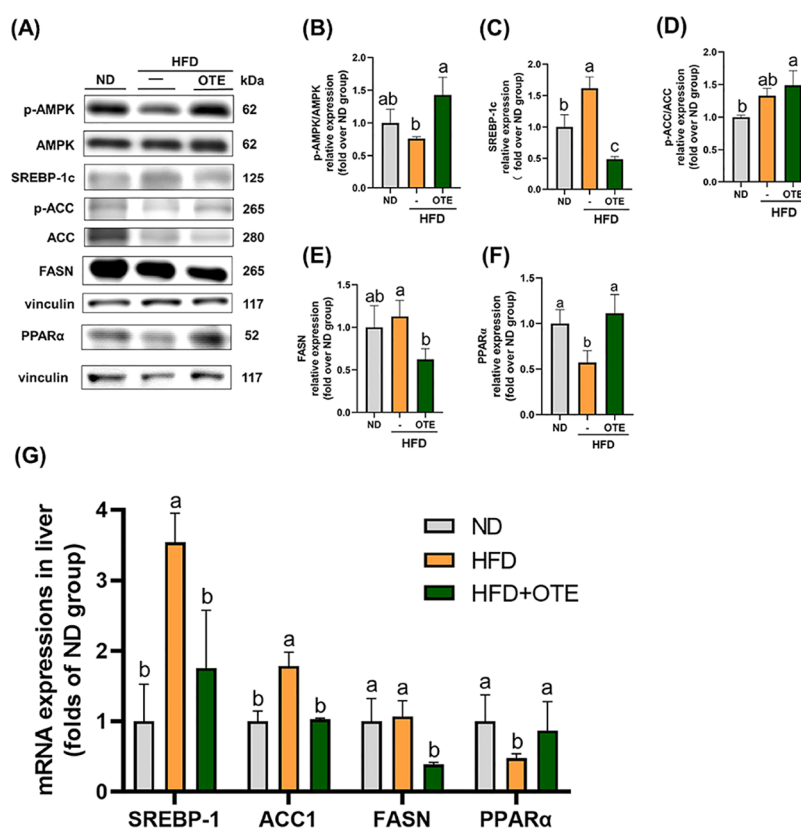


**Figure 7.** Effect of OTE supplementation on lipogenesis-related proteins, fatty acid oxidation-related proteins, and lipogenesis-related mRNA of the liver in HFD-fed C57BL/6 mice. The protein levels were analyzed by western blot, protein bands were quantified by Image J and related to hepatic de novo lipogenesis, SREBP-1, ACC1, FASN, and PPAR $\alpha$  relative mRNA expressions were evaluated by qPCR. (A) Protein levels of liver on lipogenesis-related pathway, (B) p-AMPK/AMPK protein bands, (C) SREBP-1c protein bands, (D) p-ACC/ACC protein bands, (E) FASN protein bands, (F) PPAR $\alpha$  protein bands, and (G) hepatic de novo lipogenesis related mRNA (SREBP-1, ACC1, FASN, and PPAR $\alpha$  expressions). Data are expressed as the means  $\pm$  SD ( $N = 3-4$ ). Differences were analyzed by one-way ANOVA and Duncan's multiple-range tests. The values with different letters (a–c) are significantly different ( $p < 0.05$ ) between each group.



## 4. DISCUSSION

Our study focuses on epididymal, inguinal, scapular beige adipose, and liver, and aimed to explore whether the intervention of OTE can prevent HFD-induced obesity. Previous studies have reported that GABA-fortified oolong tea has the potential to induce relaxation and diminish anxiety<sup>29</sup> and is regarded broadly as neuro-nutraceutical for improving the nervous system healthy.<sup>30</sup> Although several studies aim to explore the underlying mechanisms of the anti-obesity effects of OTE, its specific roles in lipid metabolism remain unclear.

The consumption of HFD can induce obesity in both humans and mice, and the diet-induced obesity model has become one of the most important tools to induce obesity.<sup>31</sup> Apart from that, high light intensity is also a risk factor that can cause metabolic syndrome.<sup>32</sup> Although body weight is always easier to measure, it is still not an accurate method for measuring obesity because it does not distinguish body weight from fat, bones, muscle, fluid, and so on.<sup>33</sup> Consequently, healthy people can also develop obesity-related metabolic diseases even if they are under the normal or healthy weight range.<sup>34</sup>

Food containing large amounts of fat (HFD) increases satiety and inhibits body metabolism, indicating that HFD has a negative impact on the body's metabolism.<sup>35</sup> Evidence showed that the timing of food intake affects our body metabolism through disruption of the circadian rhythm.<sup>36</sup> HFD mice have lower food and water intake but a higher food efficiency ratio and blood glucose levels, and this trend has been effectively alleviated by OTE treatment (Figure 1). OTE treatment dramatically decreased the weight of WAT, BAT, and beige adipose after feeding with HFD (Figure 2). OTE treatment reduced the weight of WAT and beige adipose by reducing the adipose cell size (Figure 2E–G). The reason is contributed to the polyphenol and the caffeine in tea. Previous studies demonstrated that caffeine stimulates lipolysis-related proteins such as HSL and ATGL and reduces the excess of fat from adipocyte cells,<sup>37</sup> consistent with our results (Figure 5). Besides, caffeine promotes thermogenesis and boosts body metabolism and energy expenditure,<sup>19</sup> similar to our results (Figure 6D). Furthermore, we found that OTE increased adiponectin levels and inhibited leptin levels in WAT, but it does not affect adiponectin levels in serum (Figure 2). Previous studies demonstrated that the transport of adiponectin depends on GGA (Golgi-localizing  $\gamma$ -adaptin ear homology ADP Ribosylation Factor-binding protein)-coated vesicles,<sup>38</sup> suggesting the possible reason that GGA protein content remains unchanged by OTE treatment, resulting in the adiponectin accumulation in adipose tissue. Another possible reason is that the adiponectin rapidly transferred from serum to the liver and is involved in hepatic de novo lipogenesis, resulting in no increase of serum adiponectin levels.

Caffeine also delays the circadian rhythm, which contributes to severe sleep problems<sup>39</sup> and increases abdominal adiposity.<sup>40</sup> We speculated that OTE is rich in caffeine that causes a reduction of adipose weight and size through lipolysis. However, caffeine also exacerbates circadian rhythm disturbances, preventing it from being absorbed into the body. In comparison, the effect of GABA on thermogenesis was not mentioned in previous studies. However, a combination of GABA with fermented *Curcuma longa* L. extract showed its anti-obesity effect via AMPK and SIRT1 activation in mice

WATs.<sup>41</sup> Moreover, the lateral hypothalamus leptin receptor activation has been reported to regulate energy homeostasis and increase body temperature in mice.<sup>42</sup> Besides, it was reported that HFD feeding might lead to decreased GABA levels in the frontal cortex and hippocampus of rats,<sup>43</sup> and meanwhile, another study suggested that an increment in brain GABA concentration might increase thermogenesis in rats.<sup>44</sup> Although GABA receptor activation is inversely correlated to UCP1 expression in humans,<sup>41</sup> the role of GABA in thermogenesis induction should be further confirmed in future studies.

NAFLD was always accompanied by the accumulation of TGs in hepatocytes, and fatty acids are considered the true lipotoxic agents.<sup>11</sup> Circadian disruption has been shown to induce neuroendocrine dysfunction and even cause NAFLD.<sup>45</sup> In our results, OTE treatment prevented hepatocellular ballooning and reduced the TG accumulation in the liver after feeding with HFD, which eventually caused a reduction in liver weight (Figure 4). There is evidence indicating that AMPK is a major regulator of body metabolism, and the activation of AMPK can strongly inhibit de novo lipogenesis in both WAT and the liver.<sup>46</sup> Our results show that OTE ameliorates fatty liver and WAT expansion by inhibiting lipogenesis-related proteins and promoting fatty acid oxidation-related proteins (Figures 5 and 7). Another study focusing on the effect of caffeine on the liver reported that caffeine is effective in reducing hepatic de novo lipogenesis by inhibition of the SREBP-1, ACC, and FASN protein expressions,<sup>18</sup> suggesting an important role in lipogenesis from the caffeine in OTE.

In conclusion, our result demonstrates that OTE treatment ameliorated lipid accumulation in adipose tissue and liver of mice induced by HFD through various mechanisms as shown in Table S2. The obesity protective property of OTE by promoting fat reduction and liver health would be beneficial to food and functional food manufacturers with the condition that OTE components must be fully further analyzed and purified in future studies.

## ■ ASSOCIATED CONTENT

### SI Supporting Information

The Supporting Information is available free of charge at <https://pubs.acs.org/doi/10.1021/acsomega.3c04874>.

Effect of OTE supplementation on body weight and indicative parameters on food consumption in HFD-fed C57BL/6 mice; summary of GABA oolong tea extracts effect on HFD-fed C57BL/6 mice (PDF)

## ■ AUTHOR INFORMATION

### Corresponding Author

Min-Hsiung Pan – Institute of Food Sciences and Technology, National Taiwan University, Taipei 10617, Taiwan; Department of Medical Research, China Medical University Hospital, China Medical University, Taichung City 40402, Taiwan; Department of Health and Nutrition Biotechnology, Asia University, Taichung City 41354, Taiwan; [orcid.org/0000-0002-5188-7030](https://orcid.org/0000-0002-5188-7030); Phone: +886-2-33664133; Email: [mhpan@ntu.edu.tw](mailto:mhpan@ntu.edu.tw); Fax: +886-2-33661771

## Authors

**Monthana Weerawatanakorn** – Department of Agro-Industry, Naresuan University, Phitsanulok 65000, Thailand

**Sang He** – Institute of Food Sciences and Technology, National Taiwan University, Taipei 10617, Taiwan

**Chun-Han Chang** – Institute of Food Sciences and Technology, National Taiwan University, Taipei 10617, Taiwan

**Yen-Chun Koh** – Institute of Food Sciences and Technology, National Taiwan University, Taipei 10617, Taiwan;

orcid.org/0000-0001-7683-873X

**Meei-Ju Yang** – Taiwan Tea Research and Extension Station, Taoyuan 326011, Taiwan

Complete contact information is available at:

<https://pubs.acs.org/10.1021/acsomega.3c04874>

## Author Contributions

M.W. and S.H. contributed equally to this study. M.H.P. and M.J.Y. conceived the idea and designed the experiments. S.H. and C.H.C. carried out the experiments, M.W., S.H., and Y.C.K. wrote the manuscript, and Y.C.K. and M.H.P. reviewed the manuscript. All authors read and approved the final manuscript.

## Funding

This work was supported by the Ministry of Science and Technology, Taiwan under Grant [110-2320-B-002-019-MY3] and was partially supported by Reinventing University Program 2023, The Ministry of Higher Education, Science, Research and Innovation (MHESI), Thailand.

## Notes

The authors declare no competing financial interest.

## REFERENCES

- (1) Sahned, J.; Mohammed Saeed, D.; Misra, S. Sugar-free workplace: a step for fighting obesity. *Cureus* **2019**, *11*, No. e6336.
- (2) Wright, S. M.; Aronne, L. J. Causes of obesity. *Abdom. Imaging* **2012**, *37*, 730–732.
- (3) WHO. *Obesity and overweight*, 2021.
- (4) Barthelemy, J.; Wolowczuk, I. Influenza A virus infection induces white adipose tissue browning: a metabolic adaptation to infection? *J. Cell. Immunol.* **2020**, *2*, 276–283.
- (5) Lopez-Jaramillo, P.; Gomez-Arbelaiz, D.; Lopez-Lopez, J.; Lopez-Lopez, C.; Martinez-Ortega, J.; Gomez-Rodriguez, A.; Triana-Cubillos, S. The role of leptin/adiponectin ratio in metabolic syndrome and diabetes. *Horm. Mol. Biol. Clin. Invest.* **2014**, *18*, 37–45.
- (6) Achari, A. E.; Jain, S. K. Adiponectin, a therapeutic target for obesity, diabetes, and endothelial dysfunction. *Int. J. Mol. Sci.* **2017**, *18*, 1321.
- (7) Leon-Cabrera, S.; Solis-Lozano, L.; Suarez-Alvarez, K.; Gonzalez-Chavez, A.; Bejar, Y. L.; Robles-Diaz, G.; Escobedo, G. Hyperleptinemia is associated with parameters of low-grade systemic inflammation and metabolic dysfunction in obese human beings. *Front. Integr. Neurosci.* **2013**, *7*, 62.
- (8) Shih, C. C.; Lin, C. H.; Wu, J. B. *Eriobotrya japonica* improves hyperlipidemia and reverses insulin resistance in high-fat-fed mice. *Phytother. Res.* **2010**, *24*, 1769–1780.
- (9) Fruhbeck, G.; Catalan, V.; Rodriguez, A.; Gomez-Ambrosi, J. Adiponectin-leptin ratio: A promising index to estimate adipose tissue dysfunction. Relation with obesity-associated cardiometabolic risk. *Adipocyte* **2018**, *7*, 57–62.
- (10) Cordeiro, A.; Costa, R.; Andrade, N.; Silva, C.; Canabrava, N.; Pena, M. J.; Rodrigues, I.; Andrade, S.; Ramalho, A. Does adipose tissue inflammation drive the development of non-alcoholic fatty liver

disease in obesity? *Clin. Res. Hepatol. Gastroenterol.* **2020**, *44*, 394–402.

(11) Berlanga, A.; Guiu-Jurado, E.; Porras, J. A.; Auguet, T. Molecular pathways in non-alcoholic fatty liver disease. *Clin. Exp. Gastroenterol.* **2014**, *7*, 221–239.

(12) Weerawatanakorn, M.; Hung, W.-L.; Pan, M.-H.; Li, S.; Li, D.; Wan, X.; Ho, C.-T. Chemistry and health beneficial effects of oolong tea and theasinensins. *Food Sci. Hum. Wellness* **2015**, *4*, 133–146.

(13) Sun, L.; Xu, H.; Ye, J.; Gaikwad, N. W. Comparative effect of black, green, oolong, and white tea intake on weight gain and bile acid metabolism. *Nutrition* **2019**, *65*, 208–215.

(14) Tung, Y. C.; Liang, Z. R.; Yang, M. J.; Ho, C. T.; Pan, M. H. Oolong tea extract alleviates weight gain in high-fat diet-induced obese rats by regulating lipid metabolism and modulating gut microbiota. *Food Funct.* **2022**, *13*, 2846–2856.

(15) Hinton, T.; Johnston, G. A. R. GABA-enriched teas as neuro-nutraceuticals. *Neurochem. Int.* **2020**, *141*, No. 104895.

(16) Hinton, T.; Jelinek, H. F.; Viengkhou, V.; Johnston, G. A.; Matthews, S. Effect of GABA-fortified oolong tea on reducing stress in a university student cohort. *Front. Nutr.* **2019**, *6*, 27–27.

(17) Quan, H. Y.; Kim, D. Y.; Chung, S. H. Caffeine attenuates lipid accumulation via activation of AMP-activated protein kinase signaling pathway in HepG2 cells. *BMB Rep.* **2013**, *46*, 207–212.

(18) Tan, X.; Sun, Y.; Chen, L.; Hu, J.; Meng, Y.; Yuan, M.; Wang, Q.; Li, S.; Zheng, G.; Qiu, Z. Caffeine ameliorates AKT-driven nonalcoholic steatohepatitis by suppressing de novo lipogenesis and MyD88 palmitoylation. *J. Agric. Food Chem.* **2022**, *70*, 6108–6122.

(19) Clark, K. S.; Coleman, C.; Shelton, R.; Heemstra, L. A.; Novak, C. M. Caffeine enhances activity thermogenesis and energy expenditure in rats. *Clin. Exp. Pharmacol. Physiol.* **2019**, *46*, 475–482.

(20) Zhang, S.; Takano, J.; Murayama, N.; Tominaga, M.; Abe, T.; Park, I.; Seol, J.; Ishihara, A.; Tanaka, Y.; Yajima, K.; Suzuki, Y.; Suzuki, C.; Fukusumi, S.; Yanagisawa, M.; Kokubo, T.; Tokuyama, K. Subacute ingestion of caffeine and oolong tea increases fat oxidation without affecting energy expenditure and sleep architecture: a randomized, placebo-controlled, double-blinded cross-over trial. *Nutrients* **2020**, *12*, 3671.

(21) Stern, J. H.; Rutkowski, J. M.; Scherer, P. E. Adiponectin, leptin, and fatty acids in the maintenance of metabolic homeostasis through adipose tissue crosstalk. *Cell Metab.* **2016**, *23*, 770–784.

(22) Pan, M. H.; Chen, J. W.; Kong, Z. L.; Wu, J. C.; Ho, C. T.; Lai, C. S. Attenuation by tetrahydrocurcumin of adiposity and hepatic steatosis in mice with high-fat-diet-induced obesity. *J. Agric. Food Chem.* **2018**, *66*, 12685–12695.

(23) Wang, J.; He, W.; Tsai, P. J.; Chen, P. H.; Ye, M.; Guo, J.; Su, Z. Mutual interaction between endoplasmic reticulum and mitochondria in nonalcoholic fatty liver disease. *Lipids Health Dis.* **2020**, *19*, 72.

(24) Zechner, R.; Kienesberger, P. C.; Haemmerle, G.; Zimmermann, R.; Lass, A. Adipose triglyceride lipase and the lipolytic catabolism of cellular fat stores. *J. Lipid Res.* **2009**, *50*, 3–21.

(25) Yau, W. W.; Yen, P. M. Thermogenesis in adipose tissue activated by thyroid hormone. *Int. J. Mol. Sci.* **2020**, *21*, 3020.

(26) Chouchani, E. T.; Kazak, L.; Spiegelman, B. M. New advances in adaptive thermogenesis: UCP1 and beyond. *Cell Metab.* **2019**, *29*, 27–37.

(27) Song, Z.; Xiaoli, A. M.; Yang, F. Regulation and metabolic significance of de novo lipogenesis in adipose tissues. *Nutrients* **2018**, *10*, 1383.

(28) Moon, Y. A. The SCAP/SREBP pathway: a mediator of hepatic steatosis. *Endocrinol. Metab.* **2017**, *32*, 6–10.

(29) Hinton, T.; Jelinek, H. F.; Viengkhou, V.; Johnston, G. A.; Matthews, S. Effect of GABA-Fortified oolong tea on reducing stress in a university student cohort. *Front. Nutr.* **2019**, *6*, 27.

(30) Hinton, T.; Johnston, G. A. R. GABA-enriched teas as neuro-nutraceuticals. *Neurochem. Int.* **2020**, *141*, No. 104895.

(31) Hariri, N.; Thibault, L. High-fat diet-induced obesity in animal models. *Nutr. Res. Rev.* **2010**, *23*, 270–299.

(32) Fan, X.; Chen, D.; Wang, Y.; Tan, Y.; Zhao, H.; Zeng, J.; Li, Y.; Guo, X.; Qiu, H.; Gu, Y. Light intensity alters the effects of light-

induced circadian disruption on glucose and lipid metabolism in mice. *Am. J. Physiol.: Endocrinol. Metab.* **2022**, *322*, E1–E9.

(33) Burkhauser, R. V.; Cawley, J. Beyond BMI: the value of more accurate measures of fatness and obesity in social science research. *J. Health Econ.* **2008**, *27*, 519–529.

(34) Dvorak, R. V.; DeNino, W. F.; Ades, P. A.; Poehlman, E. T. Phenotypic characteristics associated with insulin resistance in metabolically obese but normal-weight young women. *Diabetes* **1999**, *48*, 2210–2214.

(35) Chiazza, F.; Challa, T. D.; Lucchini, F. C.; Konrad, D.; Wueest, S. A short bout of HFD promotes long-lasting hepatic lipid accumulation. *Adipocyte* **2016**, *5*, 88–92.

(36) Asher, G.; Sassone-Corsi, P. Time for food: the intimate interplay between nutrition, metabolism, and the circadian clock. *Cell* **2015**, *161*, 84–92.

(37) Herman, A.; Herman, A. P. Caffeine's mechanisms of action and its cosmetic use. *Skin Pharmacol. Physiol.* **2012**, *26*, 8–14.

(38) Xie, L.; Boyle, D.; Sanford, D.; Scherer, P. E.; Pessin, J. E.; Mora, S. Intracellular trafficking and secretion of adiponectin is dependent on GGA-coated vesicles. *J. Biol. Chem.* **2006**, *281*, 7253–7259.

(39) Landolt, H. P. Caffeine, the circadian clock, and sleep. *Science* **2015**, *349*, 1289.

(40) Sweatt, S. K.; Gower, B. A.; Chieh, A. Y.; Liu, Y.; Li, L. Sleep quality is differentially related to adiposity in adults. *Psychoneuroendocrinology* **2018**, *98*, 46–51.

(41) Choi, M.; Mukherjee, S.; Yun, J. W. Colchicine stimulates browning via antagonism of GABA receptor B and agonism of  $\beta$ 3-adrenergic receptor in 3T3-L1 white adipocytes. *Mol. Cell. Endocrinol.* **2022**, *552*, No. 111677.

(42) de Vrind, V. A. J.; Rozeboom, A.; Wolterink-Donselaar, I. G.; Luijendijk-Berg, M. C. M.; Adan, R. A. H. Effects of GABA and leptin receptor-expressing neurons in the lateral hypothalamus on feeding, locomotion, and thermogenesis. *Obesity* **2019**, *27*, 1123–1132.

(43) Sandoval-Salazar, C.; Ramirez-Emiliano, J.; Trejo-Bahena, A.; Oviedo-Solis, C. I.; Solis-Ortiz, M. S. A high-fat diet decreases GABA concentration in the frontal cortex and hippocampus of rats. *Biol. Res.* **2016**, *49*, 15.

(44) Horton, R.; Rothwell, N. J.; Stock, M. J. Chronic inhibition of GABA transaminase results in activation of thermogenesis and brown fat in the rat. *Vasc. Pharmacol.* **1988**, *19*, 403–405.

(45) Kettner, N. M.; Voicu, H.; Finegold, M. J.; Coarfa, C.; Sreekumar, A.; Putluri, N.; Katchy, C. A.; Lee, C.; Moore, D. D.; Fu, L. Circadian homeostasis of liver metabolism suppresses hepatocarcinogenesis. *Cancer Cell* **2016**, *30*, 909–924.

(46) Garcia, D.; Hellberg, K.; Chaix, A.; Wallace, M.; Herzig, S.; Badur, M. G.; Lin, T.; Shokhirev, M. N.; Pinto, A. F. M.; Ross, D. S.; Saghatelian, A.; Panda, S.; Dow, L. E.; Metallo, C. M.; Shaw, R. J. Genetic liver-specific AMPK activation protects against diet-induced obesity and NAFLD. *Cell Rep.* **2019**, *26*, 192–208.e6.